PHYSICAL REVIEW B **92**, 041109(R) (2015)

Spin waves and spatially anisotropic exchange interactions in the $S = 2$ stripe antiferromagnet $Rb_{0.8}Fe_{1.5}S_2$

Meng Wang,[1,*] P. Valdivia,[1] Ming Yi,[1] J. X. Chen,[2] W. L. Zhang,[3] R. A. Ewings,[4] T. G. Perring,[4] Yang Zhao,[5,6] L. W. Harriger,[5] J. W. Lynn,[5] E. Bourret-Courchesne,[7] Pengcheng Dai,[8] D. H. Lee,[1,7] D. X. Yao,[2] and R. J. Birgeneau[1,7,9]

[1]*Department of Physics, University of California, Berkeley, California 94720, USA*

[2]*School of Physics and Engineering, Sun Yat-Sen University, Guangzhou 510275, China*

[3]*Institute of Physics, Chinese Academy of Sciences, P. O. Box 603, Beijing 100190, China*

[4]*ISIS Pulsed Muon and Neutron Source, STFC Rutherford Appleton Laboratory, Harwell Oxford, Didcot OX11 0QX, United Kingdom*

[5]*NIST Center for Neutron Research, National Institute of Standards and Technology, Gaithersburg, Maryland 20899, USA*

[6]*Department of Materials Science and Engineering, University of Maryland, College Park, Maryland 20742, USA*

[7]*Materials Science Division, Lawrence Berkeley National Laboratory, Berkeley, California 94720, USA*

[8]*Department of Physics and Astronomy, Rice University, Houston, Texas 77005, USA*

[9]*Department of Materials Science and Engineering, University of California, Berkeley, California 94720, USA*

(Received 24 February 2015; revised manuscript received 23 June 2015; published 13 July 2015)

An inelastic neutron scattering study of the spin waves corresponding to the stripe antiferromagnetic order in insulating $Rb_{0.8}Fe_{1.5}S_2$ throughout the Brillouin zone is reported. The spin wave spectra are well described by a Heisenberg Hamiltonian with anisotropic in-plane exchange interactions. Integrating the ordered moment and the spin fluctuations results in a total moment squared of $27.6 \pm 4.2\mu_B^2$/Fe, consistent with $S \approx 2$. Unlike XFe_2As_2 (X = Ca, Sr, and Ba), where the itinerant electrons have a significant contribution, our data suggest that this stripe antiferromagnetically ordered phase in $Rb_{0.8}Fe_{1.5}S_2$ is a Mott-like insulator with fully localized $3d$ electrons and a high-spin ground state configuration. Nevertheless, the anisotropic exchange couplings appear to be universal in the stripe phase of Fe pnictides and chalcogenides.

DOI: 10.1103/PhysRevB.92.041109 PACS number(s): 75.30.Ds, 75.50.Ee, 78.70.Nx

Superconductivity emerges in the vicinity of antiferromagnetism in both copper-based and iron-based high-transition temperature (high-T_c) superconductors [1–4]. However, the antiferromagnetism in the cuprate high-T_c and iron-based superconductors could have different origins. The parent compound of the copper oxide superconductors is a Mott insulator with $S = 1/2$ local moments [5]. In the iron pnictides, the parent compounds are bad metals with multiple bands crossing the Fermi level. The stripe antiferromagnetic (AF) ordering wave vectors coincide with the wave vectors connecting the centers of the electron and hole Fermi surfaces [6]. In fact, many view the AF order as due to the Fermi surface nesting.

From a localized point of view, with six electrons in the iron $3d$ orbitals of Fe^{2+}, the maximum total spin is $S = 2$. This spin state can be realized when the Hund's rule coupling energy J_H dominates over the crystal-field splitting associated with the FeM_4 (M = pnictigens or chalcogens) structural unit. On the other hand, a crystal-field splitting Δ_{CF} comparable to the Hund's coupling J_H can lead to an intermediate-spin $S = 1$ state. In the large crystal-field extreme, the $3d^6$ ions of Fe^{2+} will form a low-spin singlet $S = 0$ state [7–9]. In the presence of itinerant carriers the spin must be less than $S = 2$ due to charge fluctuations. Thus, the observation of $S = 2$ for Fe^{2+} would require the system to be predominately localized. Not surprisingly, the various values of ordered moments observed in different iron-based materials have been interpreted in terms of both the local moment picture and the itinerant carrier picture [7–13]. As to the value of the fluctuating local moment, inelastic neutron scattering experiments revealed an increase of S from $S \approx 1$ at 10 K to $S \approx 3/2$ at 300 K for $Fe_{1.1}Te$ and a constant $S = 1/2$ for $BaFe_2As_2$ [14–16]. In addition, an x-ray emission spectroscopy study was interpreted to imply that the iron spin state varied between $S = 0$ and 2 in the rare-earth doped $Ca_{1-x}R_xFe_2As_2$ as a function of temperature [17]. These findings suggest that the magnetism of the iron pnictides and chalcogenides should be understood from a point of view where both itinerant carriers and local moments coexist.

Recently, the discovery of 30 K superconductivity in the $A_{0.8}Fe_ySe_2$ (A = alkali metal) materials generated a great deal of research activities due to a lack of Fermi surface nesting conditions necessary for an itinerant understanding of superconducting pairing [18]. Interestingly, a stripe AF order with a rhombic iron vacancy order [Figs. 1(a) and 1(b)] was recently discovered in $K_{0.81}Fe_{1.58}Se_2$ and $Rb_{0.8}Fe_{1.5}S_2$, which are insulating compounds in proximity to the superconducting phase in this iron chalcogenide family. The stripe AF orders in these materials have strikingly similar Néel temperatures of $T_N = 280$ and 275 K, respectively, and a moment size of $M = 2.8 \pm 0.5\mu_B$ [19,20]. More importantly, this stripe AF order has the same structure as the ubiquitous magnetic order in the parent phases of iron pnictides, and has hence been proposed as a candidate parent compound for the superconducting phase in $A_{0.8}Fe_ySe_2$ [19,21]. However, previous reports on the stripe AF order always showed a mesoscopic interdigitation of the stripe AF order with a robust block AF phase with a $\sqrt{5} \times \sqrt{5}$ iron vacancy order [19,20]. Therefore, it is very important to understand the nature of this magnetic order by quantitatively characterizing the spin waves in the pure stripe AF phase.

In this Rapid Communication, we report inelastic neutron scattering studies of the spin wave excitations of the stripe

*wangm@berkeley.edu

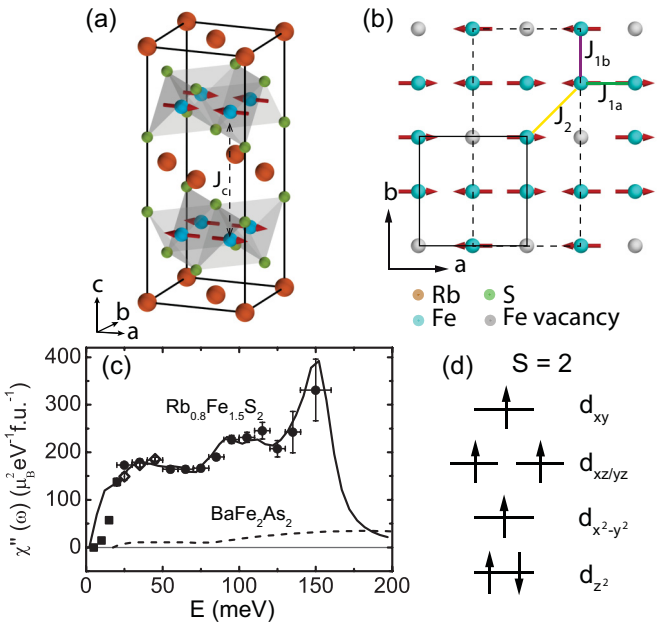

FIG. 1. (Color online) (a) Three- and (b) two-dimensional structures of the stripe AF order with rhombic iron vacancy order in $Rb_{0.8}Fe_{1.5}S_2$. We use the orthorhombic unit cell as shown by the solid square in (b) with lattice parameters of $a = 5.58$ Å, $b = 5.39$ Å, and $c = 13.889$ Å. The wave vector Q is defined as $Q = [H,K,L] = (2\pi H/a, 2\pi K/b, 2\pi L/c)$ in reciprocal lattice units (r.l.u.). The dashed rectangle is the real magnetic unit cell. (c) Dynamic susceptibility $\chi''(\omega)$ as a function of energy with $E_i = 35$ (■), 170 (◇), and 250 (●) meV at 8 K. The solid line is computed by the model discussed in the text. The dashed line is the dynamic susceptibility of $BaFe_2As_2$ from Ref. [15]. (d) A candidate for the high-spin ground state configuration of the stripe AF order [7].

AF order in insulating $Rb_{0.8}Fe_{1.5}S_2$. Only the spin excitations associated with the stripe AF order are observed in our experiment, suggesting a nearly 100% stripe AF order volume fraction. In the presence of iron vacancy order, there are six iron atoms per magnetic unit cell. Hence, one expects three doubly degenerate spin wave branches. The first acoustic and the second optical branches are observed clearly in both momentum and energy scans in our experiment. The third branch is flat in momentum space and can only be observed by scans in energy. By fitting the spin excitation spectrum to a Heisenberg Hamiltonian with spatially anisotropic exchange couplings ($SJ_{1a} = 42 \pm 5$, $SJ_{1b} = -20 \pm 2$, $SJ_2 = 17 \pm 2$, $SJ_c = 0.29 \pm 0.05$, and $SJ_s = 0.09 \pm 0.02$ meV), all of the branches of the spin excitations can be accurately described. Furthermore, the total dynamic spin fluctuation moment spectrum is calculated to be $\langle m \rangle^2 \approx 20\mu_B^2$/Fe, similar to that in the block insulating AF $Rb_{0.89}Fe_{1.58}Se_2$ [22], revealing the spin $S = 2$. Knowing that the stripe AF order is an insulator with a large charge gap (~1 eV) [23], the spin $S = 2$ suggests that all Fe 3*d* electrons are fully localized.

Our experiments were carried out on the MAPS time-of-flight (TOF) chopper spectrometer at the Rutherford-Appleton Laboratory, Didcot, U.K., and the BT-7 thermal triple-axis spectrometer at the NIST Center for Neutron Research, Gaithersburg, MD, USA. We coaligned 1.5 g of single crystals with a mosaic of 1.5° full width at half maximum for the two experiments. For the TOF experiment at MAPS, we aligned the c axis of the sample parallel to the incident beam at energies of $E_i = 35$, 80, 170, and 250 meV at 8 K. The intensities were normalized to absolute units by vanadium incoherent scattering. For the low energy neutron scattering measurements performed at BT-7, we fixed the final energy at 14.7 meV, with horizontal collimations of open-$80' - S - 80' - 120'$, where S = sample, and two pyrolytic graphite filters after the sample [24]. Uncertainties where indicated represent one standard deviation.

We show spin excitations in the $[H,K]$ plane at various energies in Figs. 2(a)–2(e). The spin excitations stem from the AF wave vectors, disperse outwards, and separate into two arcs at 65 ± 5 (this notation represents the signal averaged over $60 < E < 70$ meV) and 75 ± 5 meV. At the energy of 110 ± 9 meV, the wave vectors rotate 90°.

To describe the spin waves in $Rb_{0.8}Fe_{1.5}S_2$, we employed a Heisenberg model with in-plane nearest-neighbor (J_{1a}, J_{1b}) and next-nearest-neighbor (J_2) exchange couplings, together with the coupling between layers, J_c, as shown in Figs. 1(a) and 1(b), and the single ion anisotropy term, J_s. The Hamiltonian can be written as

$$\hat{H} = \frac{J_{r,r'}}{2} \sum_{r,r'} \mathbf{S}_r \cdot \mathbf{S}_{r'} - J_s \sum_r \left(\mathbf{S}_r^z\right)^2, \qquad (1)$$

where $J_{r,r'}$ are the effective exchange couplings and (r,r') label the iron sites [25]. The spin wave excitation spectrum can be expressed analytically by solving Eq. (1) using the linear spin wave approximation [11,13,16,22]. We performed resolution convoluted fits to the time-of-flight data using the TOBYFIT program [26]. From the best fit to the experimental data, the parameters were determined to be $SJ_{1a} = 42 \pm 5$, $SJ_{1b} = -20 \pm 2$, and $SJ_2 = 17 \pm 2$ meV, and for computational convenience an energy independent damping $\Gamma = 7 \pm 2$ meV. The widths of the spin wave peaks in H and K were close to being instrumental resolution limited, as expected for an insulator; this also holds true for $K_{0.81}Fe_{1.58}Se_2$ [27,29]. The simulations with the fit parameters at the identical energies of Figs. 2(a)–2(e) are presented in Figs. 2(f)–2(j).

To compare quantitatively the experimental data with the model, we plot cuts along the $[H,0]$ and $[1,K]$ directions and compare the cuts with the best fits for a wide range of energies in Fig. 3. The fits are in good agreement with the experimental data at all energies. The small discrepancy near $Q = (2,0)$ is due to an acoustic phonon. The weaker and flatter cut along the $[1,K]$ direction at 65 ± 5 meV in Fig. 3(g) and the cut along the $[H,0]$ direction at 110 ± 9 meV in Fig. 3(d) are consistent with the splitting of the first branch along the $[H,0]$ direction and the 90° rotation of the second branch.

Figures 4(a) and 4(b) show the dispersion relations along the $[H,0]$ and $[1,K]$ directions with $E_i = 250$ meV at 8 K, respectively. The spin excitations from the second twin at $Q = (0.5,0), E = 25$ meV in Fig. 4(a) and the second branch of spin excitations at energies between 90 and 120 meV in Fig. 4(b) can be observed. The dispersion of the spin excitations extracted from extensive constant energy cuts and Q cuts, together with the results of simulations with the best fit parameters, are plotted in Figs. 4(c) and 4(d). Three branches of spin excitations can be seen. We tried to fit the

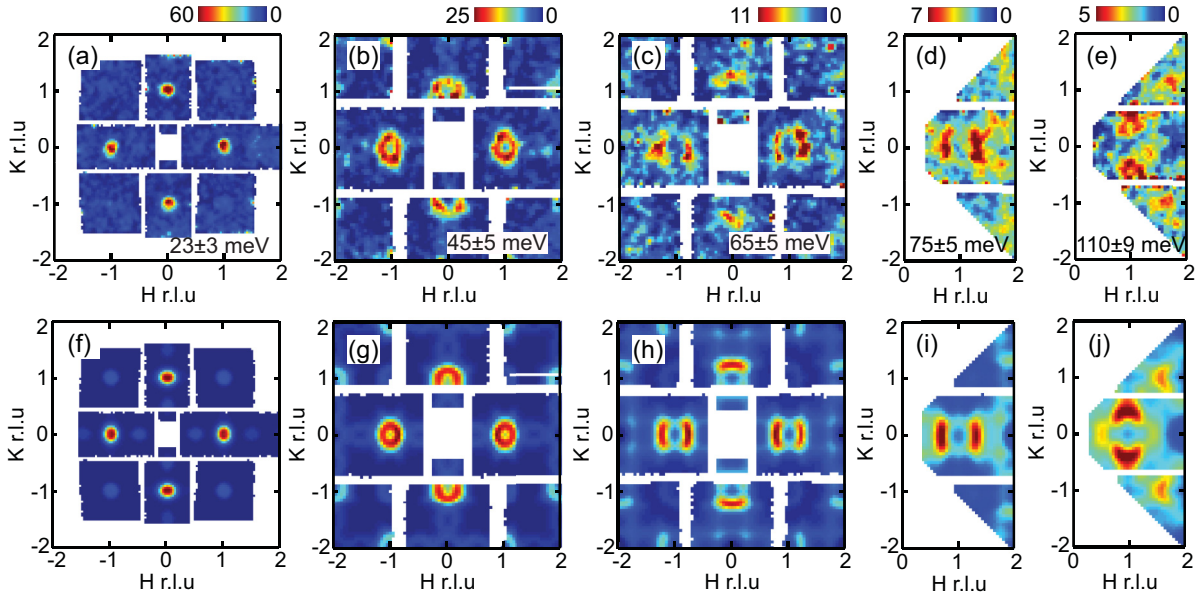

FIG. 2. (Color online) Constant energy slices in the $[H,K]$ plane of the spin waves averaged at energies of (a) 23 ± 3 meV with $E_i = 80$ meV, and (b) 45 ± 5, (c) 65 ± 5, (d) 75 ± 5, (e) 110 ± 9 meV with $E_i = 250$ meV, all at 8 K. (f)–(j) Simulations of spin excitations at the identical energies as in (a)–(e) using the exchange couplings from the best fits to the experimental data. The simulations were convoluted with the instrumental resolution. The color bar is the same for each energy transfer in units of mb Sr^{-1} meV^{-1} $\mathrm{f.u.}^{-1}$.

dispersions in $Rb_{0.8}Fe_{1.5}S_2$ with the parameters obtained for $K_{0.81}Fe_{1.58}Se_2$ [27]. The dispersions of the first branch along the $[H,0]$ and $[1,K]$ directions were matched very well, but the second branch along the $[1,K]$ direction deviated from the experimental data (see the Supplemental Material [28]).

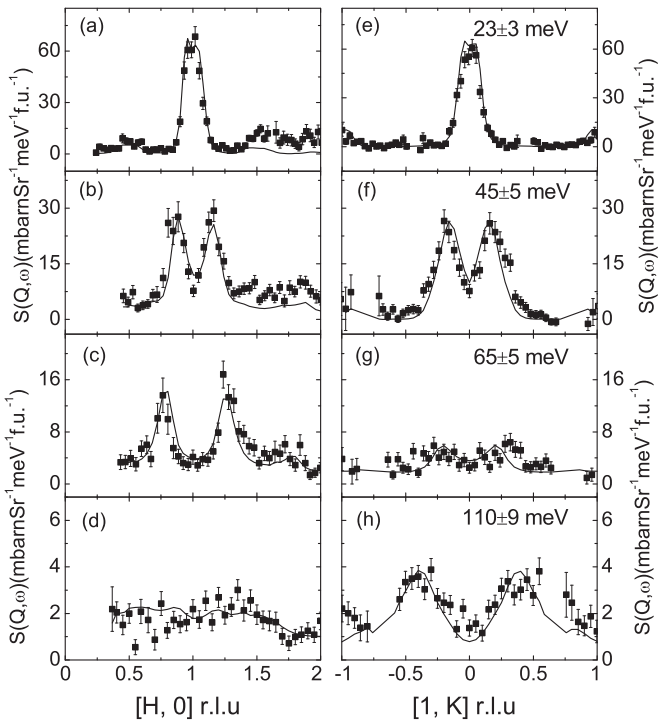

FIG. 3. Constant energy cuts through $Q = (1,0)$ along the (a)–(d) $[H,0]$ and (e)–(h) $[1,K]$ directions averaged at energies of 23 ± 3 meV with $E_i = 80$ meV, and 45 ± 5, 65 ± 5, and 110 ± 9 meV with $E_i = 250$ meV, at 8 K. The solid lines are the best fits obtained from the TOBYFIT program.

In order to determine the exchange coupling between layers, J_c, and the single-ion anisotropy term, J_s, we measured the L modulation of the low energy spin excitations at 2 K. The measurements show that a gap in the spin excitations opens up below $\Delta = 6$ meV and that J_c only affects the spin excitation spectrum below 15 meV [Fig. 4(e)]. By fitting the L-modulated spin excitation spectrum, we determined $SJ_c = 0.29 \pm 0.05$ and $SJ_s = 0.09 \pm 0.02$ meV. The temperature dependence of the spin gap was also studied and is presented in Fig. 4(f). The spin gap remained sharp right up to the phase transition. The scaled magnetic order parameter is plotted along with the temperature dependent spin gap. The evolution of the spin gap with temperature follows the trend of the AF order, in agreement with the behavior observed in K_2NiF_4, a quasi-two-dimensional (2D) Heisenberg AF insulator [29].

To unveil the spin state in the stripe AF order of $Rb_{0.8}Fe_{1.5}S_2$, we examined the sum rule of the magnetic neutron scattering. One can calculate the total fluctuating moment squared $\langle \mathbf{m}^2 \rangle$ by integrating the susceptibility $\chi''(\mathbf{q},\omega)$ over the bandwidth of the spin excitations via

$$\langle \mathbf{m}^2 \rangle = \frac{3\hbar}{\pi} \int_{-\infty}^{+\infty} \frac{\int \chi''(\mathbf{q},\omega) d\mathbf{q} / \int d\mathbf{q}}{1 - \exp(-\hbar\omega / k_B T)} d\omega. \qquad (2)$$

The total moment sum rule is $M_0^2 = g^2 M^2 + \langle \mathbf{m}^2 \rangle = g^2 S(S+1)$, where g is the Landé g factor and M is the static moment. Thus the spin S can be extracted [22,30,31].

The averaged dynamic susceptibility in a Brillouin zone $\chi''(\omega) = \int \chi''(\mathbf{q},\omega) d\mathbf{q} / \int d\mathbf{q}$ is plotted in Fig. 1(c). The spin fluctuations in $Rb_{0.8}Fe_{1.5}S_2$ are obviously stronger than those in $BaFe_2As_2$. Integrating the dynamic susceptibility through all the spin excitation bandwidths results in $29.7 \pm 5.5 \mu_B^2$/formula unit (f.u.), and thus $19.8 \pm 3.7 \mu_B^2$/Fe. Taking the ordered moment $M = 2.8 \pm 0.5 \mu_B$ into account, the total moment squared per Fe is $27.6 \pm 4.2 \mu_B^2$, which,

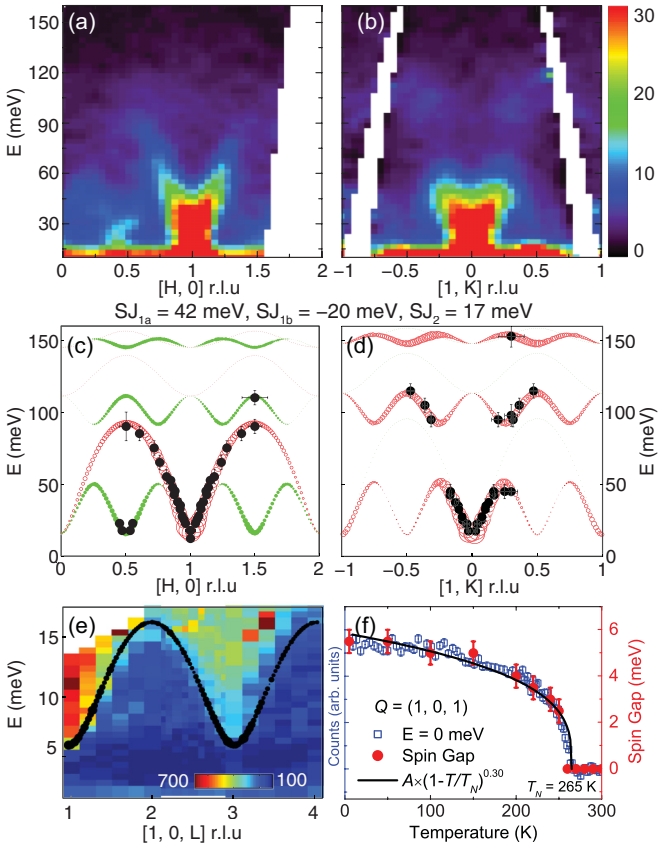

FIG. 4. (Color online) (a) Spin excitations along the $[H,0]$ direction, averaging over $K = \pm 0.2$ r.l.u. and (b) along the $[1,K]$ direction, averaging over $H = 1 \pm 0.2$ r.l.u. with $E_i = 250$ meV at 8 K. (c), (d) The dispersion extracted from experimental data and simulations with the best fit parameters. The red circles are from the first twin, and the green circles are from the second twin (see the Supplemental Material). The intensity of the simulations is proportional to $\chi''(\mathbf{q},\omega) \times \sqrt{E}$. (e) The L modulation of the low energy spin excitations at 2 K and simulations with $SJ_c = 0.29$, $SJ_s = 0.09$ meV. The intensity is proportional to $\chi''(\mathbf{q},\omega)$. (f) The temperature evolution of the spin gap measured at $Q = (1,0,1)$. The solid line is the result of a fit to the magnetic order parameter (the blue squares) with $A(1 - T/T_N)^{\beta}$, where A is a scaler, $T_N = 265$ K, and $\beta = 0.30$.

assuming $g = 2.0$, results in a spin $S = 2.2 \pm 0.2$, which is equal to the upper limit of $24\mu_B^2$ and $S = 2$ as the Hund's rule result for the $3d$ Fe^{2+} within the error. The results reveal that to within the errors all six $3d$ electrons of Fe^{2+} are associated with the local moment in the high-spin state. A candidate spin configuration is illustrated in Fig. 1(d). The fact that the carriers are fully localized in $Rb_{0.8}Fe_{1.5}S_2$ is consistent with our photoemission measurements on several pieces of single crystals from the same batch. These measurements also reveal a large charge gap below the Fermi energy, suggesting that the stripe AF phase is a Mott-like insulator with the integer spin $S = 2$ [21,32], rather than a small gap band insulator [19,20,33]. The Mott localization in $Rb_{0.8}Fe_{1.5}S_2$ is realized by the presence of the rhombic iron vacancy order, which has enlarged the in-plane Fe-Fe distance, and thus enhanced the correlation [21,32].

TABLE I. The magnetic exchange couplings and spin states in the stripe AF order of iron pnictides and chalcogenides [13,16,27].

Compounds	SJ_{1a}	SJ_{1b}	SJ_2 (meV)	S	M (μ_B)	T_N (K)
$CaFe_2As_2$	50(10)	−6(5)	19(4)	1/2	0.80	173
$BaFe_2As_2$	59(2)	−9(2)	14(1)	1/2	0.87	143
$SrFe_2As_2$(L)	31(1)	−5(5)	22(1)	0.30	0.94	220
$SrFe_2As_2$(H)	39(2)	−5(5)	27(1)	0.69	0.94	220
$K_{0.85}Fe_{1.54}Se_2$	38(7)	−11(5)	19(2)		2.8	280
$Rb_{0.8}Fe_{1.5}S_2$	42(5)	−20(2)	17(2)	2	2.8(0.5)	265

Several theoretical methods have been successfully explored to describe the spin waves of the stripe AF order: a combination of density functional theory (DFT) and dynamic mean field theory (DMFT) [34,35]; a Heisenberg model with anisotropic in-plane exchange couplings $J_{1a}(>0)$, $J_{1b}(<0)$, and J_2 [11,13,16,27]; and a Heisenberg model with J_1, J_2 and a large biquadratic coupling K [10,36,37]. The spin waves of $Rb_{0.8}Fe_{1.5}S_2$ could be described by either model. In particular, the rhombic iron vacancy order which has already broken the C_4 symmetry forms at a temperature higher than 718 K [20]. The anisotropic J_{1a} and J_{1b} in $Rb_{0.8}Fe_{1.5}S_2$ could originate from structural orthorhombicity and possible orbital ordering [38]. For the $J_1 - J_2 - K$ model, the exchange couplings are estimated to be $J_1 S = (J_{1a} + J_{1b})S/2 = 11 \pm 3$, $J_2 S = 17 \pm 2$, and $KS = (J_{1a} - J_{1b})S/4 = 15.5 \pm 1.4$ meV [36]. The biquadratic term could be enhanced by the dynamic fluctuations in the chalcogen height. Distinguishing the two models microscopically is beyond the scope of this work.

We list in Table I the fitted magnetic exchange couplings and measured Fe spin values in a number of stripe phase Fe arsenides and chalcogenides. The Fermi surfaces in these materials vary significantly, as do, concomitantly, the conductivity, the ordered moments, and the effective spin values. In spite of this, the exchange couplings measured in units of SJ are remarkably universal. This result is both striking and mysterious. It remains to be seen how this relates to the superconductivity of the iron chalcogenides.

In summary, we have studied the spin waves of the pure stripe AF order in $Rb_{0.8}Fe_{1.5}S_2$ over a wide range in reciprocal space and energy. Our inelastic neutron scattering data reveal that even though the stripe AF order has strikingly similar SJ with all the other iron pinctides and chalcogenides, it is an ideal $S = 2$ Heisenberg antiferromagnet with fully localized moments exhibiting Mott insulator behavior. This indicates the importance of strong electron correlations in iron-based superconductors, which have thus far mostly been understood from an itinerant point of view. Our results hence form a bridge that connects the iron-based superconductors to the cuprates.

We thank Qimiao Si, Yao Shen, and Jun Zhao for useful discussions. This work is supported by the Director, Office of Science, Office of Basic Energy Sciences, U.S. Department of Energy, under Contract No. DE-AC02-05CH11231 and the office of Basic Energy Sciences U.S. DOE Grant No. DE-AC03-76SF008. We also acknowledge support from NBRPC-2012CB821400 and NSFC-11275279. Work at Rice is supported by the U.S. DOE, BES under Contract No. DE-SC0012311 (P.D.).

[1] M. A. Kastner, R. J. Birgeneau, G. Shirane, and Y. Endoh, Rev. Mod. Phys. **70**, 897 (1998).
[2] R. J. Birgeneau, C. Stock, J. M. Tranquada, and K. Yamada, J. Phys. Soc. Jpn. **75**, 111003 (2006).
[3] D. Johnston, Adv. Phys. **59**, 803 (2010).
[4] P. C. Dai, J. P. Hu, and E. Dagotto, Nat. Phys. **8**, 709 (2012).
[5] S. M. Hayden, G. Aeppli, H. A. Mook, T. G. Perring, T. E. Mason, S. W. Cheong, and Z. Fisk, Phys. Rev. Lett. **76**, 1344 (1996).
[6] J. Dong *et al.*, Europhys. Lett. **83**, 27006 (2008).
[7] Q. Si and E. Abrahams, Phys. Rev. Lett. **101**, 076401 (2008).
[8] F. Krüger, S. Kumar, J. Zaanen, and J. van den Brink, Phys. Rev. B **79**, 054504 (2009).
[9] K. Haule and G. Kotliar, New J. Phys. **11**, 025021 (2009).
[10] D. Stanek, O. P. Sushkov, and G. S. Uhrig, Phys. Rev. B **84**, 064505 (2011).
[11] J. Zhao *et al.*, Nat. Phys. **5**, 555 (2009).
[12] S. O. Diallo *et al.*, Phys. Rev. Lett. **102**, 187206 (2009).
[13] R. A. Ewings, T. G. Perring, R. I. Bewley, T. Guidi, M. J. Pitcher, D. R. Parker, S. J. Clarke, and A. T. Boothroyd, Phys. Rev. B **78**, 220501(R) (2008); R. A. Ewings, T. G. Perring, J. Gillett, S. D. Das, S. E. Sebastian, A. E. Taylor, T. Guidi, and A. T. Boothroyd, *ibid.* **83**, 214519 (2011).
[14] I. A. Zaliznyak, Z. Xu, J. M. Tranquada, G. Gu, A. M. Tsvelik, and M. B. Stone, Phys. Rev. Lett. **107**, 216403 (2011).
[15] M. S. Liu *et al.*, Nat. Phys. **8**, 376 (2012).
[16] L. W. Harriger, H. Q. Luo, M. S. Liu, C. Frost, J. P. Hu, M. R. Norman, and P. Dai, Phys. Rev. B **84**, 054544 (2011); L. W. Harriger, M. Liu, H. Luo, R. A. Ewings, C. D. Frost, T. G. Perring, and P. Dai, *ibid.* **86**, 140403(R) (2012).
[17] H. Gretarsson, S. R. Saha, T. Drye, J. Paglione, J. Kim, D. Casa, T. Gog, W. Wu, S. R. Julian, and Y. J. Kim, Phys. Rev. Lett. **110**, 047003 (2013).
[18] E. Dagotto, Rev. Mod. Phys. **85**, 849 (2013).
[19] J. Zhao, H. Cao, E. Bourret-Courchesne, D. H. Lee, and R. J. Birgeneau, Phys. Rev. Lett. **109**, 267003 (2012).
[20] M. Wang, W. Tian, P. Valdivia, S. Chi, E. Bourret-Courchesne, P. Dai, and R. J. Birgeneau, Phys. Rev. B **90**, 125148 (2014).
[21] R. Yu, J. X. Zhu, and Q. Si, Phys. Rev. Lett. **106**, 186401 (2011); R. Yu and Q. Si, *ibid.* **110**, 146402 (2013).
[22] M. Y. Wang *et al.*, Nat. Commun. **2**, 580 (2011).
[23] F. Chen *et al.*, Phys. Rev. X **1**, 021020 (2011).
[24] J. W. Lynn *et al.*, J. Res. Natl. Inst. Stand. Technol. **117**, 61 (2012).
[25] D. X. Yao and E. W. Carlson, Front. Phys. China **5**, 166 (2010).
[26] T. G. Perring *et al.*, http://tobyfit.isis.rl.ac.uk.
[27] J. Zhao, Y. Shen, R. J. Birgeneau, M. Gao, Z. Y. Lu, D. H. Lee, X. Z. Lu, H. J. Xiang, D. L. Abernathy, and Y. Zhao, Phys. Rev. Lett. **112**, 177002 (2014).
[28] See Supplemental Material at http://link.aps.org/supplemental/10.1103/PhysRevB.92.041109 for simulations of spin waves for each twin in $Rb_{0.8}Fe_{1.5}S_2$ and a comparison with the simulated spin waves with the parameters obtained in $K_{0.81}Fe_{1.58}Se_2$.
[29] R. J. Birgeneau, J. Skalyo, and G. Shirane, Phys. Rev. B **3**, 1736 (1971).
[30] C. Lester, J. H. Chu, J. G. Analytis, T. G. Perring, I. R. Fisher, and S. M. Hayden, Phys. Rev. B **81**, 064505 (2010).
[31] J. Lorenzana, G. Seibold, and R. Coldea, Phys. Rev. B **72**, 224511 (2005).
[32] C. Cao and J. H. Dai, Phys. Rev. B **83**, 193104 (2011).
[33] X. W. Yan, M. Gao, Z. Y. Lu, and T. Xiang, Phys. Rev. Lett. **106**, 087005 (2011).
[34] Z. P. Yin, K. Haule, and G. Kotliar, Nat. Phys. **10**, 845 (2014).
[35] C. Zhang *et al.*, Phys. Rev. Lett. **112**, 217202 (2014).
[36] A. L. Wysocki, L. D. Belashchenko, and V. P. Antropov, Nat. Phys. **7**, 485 (2011).
[37] R. Yu, Z. Wang, P. Goswami, A. H. Nevidomskyy, Q. Si, and E. Abrahams, Phys. Rev. B **86**, 085148 (2012).
[38] W. Lv, F. Kruger, and P. Phillips, Phys. Rev. B **82**, 045125 (2010).